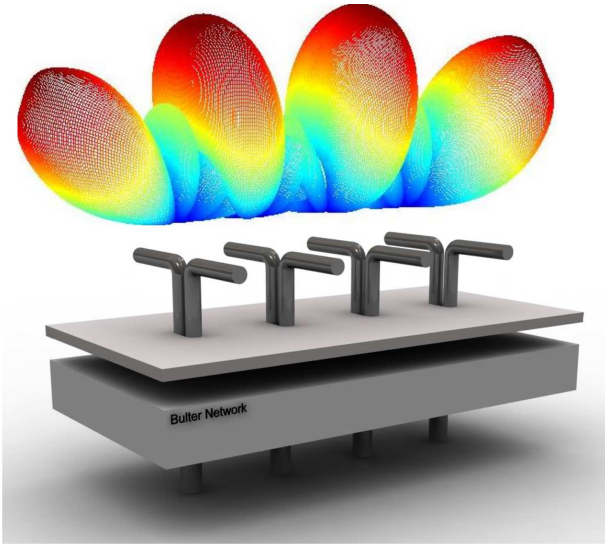

Spatial Characterization of Multi-element Antennas

Nima Jamaly

Department of Signals and Systems
CHALMERS UNIVERSITY OF TECHNOLOGY
Gothenburg, Sweden 2011

Thesis for the degree of Licentiate of Engineering

Spatial Characterization of Multi-element Antennas

by

Nima Jamaly

CHALMERS

Department of Signals and Systems
Antenna Group
Chalmers University of Technology
Gothenburg, Sweden 2011

Spatial Characterization of Multi-element Antennas

Nima Jamaly

This thesis has been prepared using LaTeX.

Technical Report No. R002/2011
School of Electrical Engineering
Chalmers University of Technology
ISSN 1403-266X

Department of Signals and Systems
Chalmers University of Technology
SE-412 96 Gothenburg, Sweden

Phone: +46 (0)31 772 4827
Fax: +46 (0)31 772 1748
E-mail: jamaly@chalmers.se

Printed by Chalmers Reproservice
Gothenburg, Sweden, February 2011

To the undying memory of my dears "ammeh"
Mansoureh and "amoo" H. Nobakht.

Foreword

The overall goal of the current thesis is to establish some bases for understanding and characterization of multi-port antennas in a rich multipath environment. Multi-port antennas are the inevitable keystone of Multiple Input and Multiple Output (MIMO) wireless communication systems. Due to multidisciplinary nature of the applications of multi-element antennas, they are the subjects of many research groups worldwide resulting in inconsistent nomenclature among them. In this report, much effort is expended to look upon this realm of engineering in a unifying approach, with the major stress on electromagnetic aspects of this area.

Advantages in using multi-port antennas have been presented in different ways and are available in numerous references. Yet, before entering into the heart of the current thesis, we shall briefly stress the pros in application of these radiation terminals to motivate their analysis. This is the main focus of the first chapter. On the other hand, the global concern of this report is characterization of multi-port antennas more for their benefits in multipath environments. Not only does this characterization depend on electromagnetic (EM) properties of these radiation systems, but also it relies on the features of the incoming EM waves associated to the multipath environment. The latter is addressed in the last part of the first chapter. Chapter 2 throws light upon different significant parameters as the key-gauges for characterization of multi-port antennas. In this regard, it requires a special care.

Received signals at different ports of a multi-element antenna in a multipath environment are the main sources for its assessment. There are certain functions governing the relation between the received signals at different ports of a radiation system and an arbitrary incident EM wave. Certainly, the mentioned functions are pendant on EM properties of the pertinent antennas too. The precise derivation of these formulas for different cases of interest, as a discipline of its own, establishes the third chapter.

The foundations created in the aforementioned chapters are the bases of a software called Multipath environment Emulator for performance Simulation of radiation Terminals (MEST). The simulation process for this software is elaborated in Chapter 4. There are several examples in this chapter for verification of the results produced by MEST. Finally, a brief chapter will address some overall points regarding the appended papers in this thesis. The second part of the report is dedicated to the published papers whose layouts have been changed to go well with the first part of the thesis.

Keywords: Beam-forming technique, beam-port, Butler network, capacity, correlation, decoupling efficiency, diversity gain, element port, embedded radiation efficiencies, isotropic environment, multipath environments (fading environments), multi-port (multi-element)

antennas (radiation terminals), received port signals.

Acknowlegments

I would like to first thank my supervisors for their time and patience. Prof. Per-Simon Kildal is appreciated for his kind supports. I express my sincere thanks to Prof. Jan Carlsson for his brilliant and instructive discussions. I am profoundly grateful to Prof. Yahya Rahmat-Samii for his kindness and the time he dedicated to the progress of my education.

I also express my most sincere acknowledgements to Prof. Mats Viberg, the former head of the division, and Prof. Erik Ström for their constant support and patience. Prof. D. Yazdanfar is appreciated for his kind advices and encouragements. In the last few years, I was the beneficiary of an excellent opportunity to be under guidance of highly renowned professors worldwide: Professors W. Wiesbeck, J. Mosig, A. Kishk, and U. Westergren. You are, by all means, unique and have my profound respect forever. My dear professors, Thomas Rylander and Eva Rajo are also kindly appreciated.

This thesis has been supported by the Swedish Governmental Agency for Innovation Systems (VINNOVA) within the VINN Excellence Centre Chase at Chalmers. The collaboration of different companies like Sony Ericsson Mobile Communications and Perlos AB within framework of MIMO Terminal project has been highly beneficial. A special mention goes to Ingmar Karlsson, the former Chase center manager, for his kindness and creating a great circumstance for research and innovation. I am also deeply indebted to all permanent staff of S2, in particular, my dears Lars Börjesson, Agneta Kinnander, Gunilla Walther and Ann-Christine Lindbom. Your kindness will never disappear from my memories.

My special thanks to all former and current members of the Antenna group. You are deep in my heart. I am proud of many resourceful Iranian PhD students in S2. My most sincere gratefulness to all of you for creating an unforgettable period in my life. Cheers to you all. My ladies, N. Mohammad-Gholizadeh and S. Shahsavari are appreciated for the invaluable helps they made in preparation of this thesis. Last but not least, I would like to mention the unfailing support of my respectable family, with love of whom I live and breathe. Warm thanks to you and your love, which inspires me the most.

List of Appended Papers

Paper I
N. Jamaly, P.-S. Kildal and J. Carlsson, "Compact Formulas for Diversity Gains of Two-port Antennas," *IEEE Antennas and Wireless Propagation Letters*, vol. 9, pp. 970-973, 2010.

Paper II
N. Jamaly, H. Zhu, P.-S. Kildal and J. Carlsson, "Performance of Directive Multi-element Antennas versus Multi-beam Arrays in MIMO Communication Systems," in *Proceedings of the Fourth European Conference on Antennas and Propagation (EuCAP)*, 2010, pp. 1-5.

Paper III
N. Jamaly, C. Gómez-Calero, P.-S. Kildal, J. Carlsson and A. Wolfgang, "Study of Excitation on Beam Ports versus Element Ports in Performance Evaluation of Diversity and MIMO Arrays," in *Proceedings of the Third European Conference on Antennas and Propagation (EuCAP)*, 2009, pp. 1753-1757.

Paper IV
Y. B. Karandikar, D. Nyberg, N. Jamaly, and P.-S. Kildal, "Mode Counting in Rectangular, Cylindrical and Spherical Cavities with Application to Wireless Measurements in Reverberation Chambers," *IEEE Transactions on Electromagnetic Compatibility*, vol. 5, pp. 1044-1046, 2009.

Paper V
C. Gómez-Calero, N. Jamaly, L. Gonzlez and R. Martnez, "Effect of Mutual Coupling and Human Body on MIMO Performance," in *Proceedings of the Third European Conference on Antennas and Propagation (EuCAP)*, 2009, pp. 1042-1046.

Contents

Acronyms

ADG	Apparent Diversity Gain
AoA	Angle of Arrival
CDF	Cumulative Distribution Function
EDG	Effective Diversity Gain
EM	Electromagnetic
MEST	Multipath environment Emulator for performance Simulation of radiation Terminals.
MIMO	Multiple Input and Multiple Output
MRC	Maximum Ratio Combining
PDF	Probability Density Function
PEC	Perfect Electric Conductor
SC	Selection Combining
SNR	Signal-to-Noise Ratio
ST	Space-Time
TEM	Transverse Electromagnetic
WSAP	Wire Structure Analysis Program

Part I
Analysis & Formulation

Chapter 1

Multi-port Antennas in Multipath Environments

Usage of multiple antennas in multipath environments has long been of concern for advantages it renders. The very first benefit of multiple antennas was recognized as the array gain they offer. In particular, after an extensive study in 1970s based upon the notion of space diversity, they attracted considerable amount of attention. Afterwards, in late 80s and early 90's, spatial multiplexing has been introduced by communication engineers which revealed a further significant advantage of them in increasing the capacity (or if you like, spectral efficiency) of a wireless communication system. For the time being, we shall dedicate a few minutes giving a brief introduction on the benefits of multi-element radiation terminals at the transmitter and the receiver sides similar to those listed in [1].

The first advantage of multi-port antennas in communication systems is the *Array Gain*. Array gain is referred to an average enhancement in received SNR at the receiver as a result of coherent combining of signals at the ports of the receiver terminal or the transmitter. Signals received at different ports have different amplitudes and phases and when combined coherently can bestow enhanced SNR being proportional to the number of the present elements. In contrast, exploitation of array gain for the case wherein a multi-element antenna is used at the transmitter requires the knowledge of the channel at this side. The latter is beyond the scope of this thesis and, thus, will not be discussed here. A further recognized benefits of these systems are shown by *Diversity Gain*. This concept will be addressed in the following chapter. Yet, for the time being, to briefly touch this issue, just recall that fluctuation in the received signal power in a multipath environment is called *fading*. When the power of a signal drops significantly, it is said to be *in fade* resulting in a loss of connection. Diversity gain is used in wireless communication systems to combat fading. In addition to that is the *Spatial Multiplexing* which for the same bandwidth offers a linear increase in the transmission rate without any power expenditure. For instance, a bit stream to be transmitted can be demultiplex into two half-rate sub-streams, and transmitted through different antenna simultaneously. Under a suitable channel conditions, the spatial signatures of these signals at the receiver terminal are well separated. Hence, the receiver having the knowledge of the channel can differentiate between these two co-channel signals and extract the corresponding sub-streams accordingly. Moreover, *Interference Reduction* was mentioned as the last advantage of

these systems. It happens due to frequency reuse in wireless channels. When multi-element antennas are used, the difference between the spatial signatures of the signals of same frequency makes it possible to reduce the interference between them.

A simple look at the schematic of a Space-Time (ST) wireless communication system reveals that the differences between a ST communication system and a conventional system are limited to three different parts. That is, ST-coding/interleaving, ST-prefilterning, and finally multi-element radiation terminals which is the main concern of the current thesis. In what follows we are going to carefully study the performance of a multi-element antenna and to investigate the different gauges by which they have been characterized. Moreover, we would like to see whether we could directly realize system parameters given above for these radiation systems. Please bear in mind that we are looking upon these antennas from electromagnetics (EM) standpoint.

1.1 Conventional versus Contemporary Characterization of Antennas

In conventional characterization of antennas, the radiation pattern plays a central role. Perhaps the main job of antenna engineers has been to architecture the radiation pattern to meet the desired specification. Parameters like half power beam width, beam width between first nulls, side lobe level, back-lobe level, directivity, and polarization are indeed the direct derivatives of the radiation pattern. Also, some other parameters like input impedance, bandwidth, radar cross section, size, weight etc. are of considerable importance.

Yet, in contemporary design of the radiation systems, which are going to be used in multipath environment (e.g., NLOS)[1], the radiation pattern of an antenna loses its central role and hence architecture of the radiation pattern is not the main concern of the antenna engineers. As a matter of fact, the ultimate concerns of the antenna engineers are to design antennas which not only meet the system considerations e.g., size and weight, but also exhibit, in general, acceptable total embedded radiation efficiencies.

The major difference between characterization of antennas in LOS[2] and in NLOS resides on the fact that while the pattern of an antenna is the main source in LOS frame, the received signal at the port of an antenna is the unique source to be used for that purpose. For instance, the mean received power, which plays a significant role in characterization of antennas, is the average power at the port of an antenna measured in a multipath environment.[3] Furthermore, at the presence of multi-port antenna which has different radiation elements placed close to each other, a different term called *correlation* has been coined. Correlation between two elements (or ports) of an antenna system is the cross-correlation between the received signals at those ports. Hence, to characterize a multi-element antenna in multipath environments, we need to either measure the antenna's port signal in a real multipath environment or create a simulation tool, which can fulfill the same task. The measurement of an antenna has always its own challenges among

[1] None line-of-sight cases
[2] Line-of-sight
[3] Refer to Chapter 4 on page 27.

which the repeatability of the same environment stands out. This is beyond the scope planned for this thesis, yet for the time being just bear in mind that a new generation of measurement tools has been used for this purpose called Reverberation Chambers which are limited to a particular type of environments of certain characteristics.

In the frame of this thesis, our main goal is to create a simulation tool by which we could create the samples of received signals at the ports of a multi-element terminal operating in a multipath environment. In the next few chapters, the bases of such a software are established and well detailed to a point of satisfaction. On our way to this end, before anything we state that the received signal at the port of a radiation terminal, in general, depends on two major factors. On one side, it depends on the properties of the multipath environment which are the characteristics of the incoming EM waves. And, on the other side, it relies on EM characteristics of the antenna. The latter is the subject of the third chapter, whereas the former is clarified to some extent in the following subsection.

1.2 Properties of Incoming EM waves in Multipath Environments

As long as the characteristics of the incoming EM waves are concerned, there shall be polarization as well as amplitude and phase description. Furthermore, the received signals at the ports of a multi-element antenna depend on the incident direction of the incoming EM waves, known as Angle of Arrival (AoA), too. The latter was the focus of many papers in which different non-uniform models, at least for elevation plane, have been purposed [2]-[8], and the interested reader is referred to these references.[4]

Having said that, it is also rewarding for us to note that concentrating solely on the distribution of AoA in an environment is obviously lacking inasmuch as it does not take into account the orientation of the radiation terminal having presumably a non-uniform gain pattern. Therefore, for any single orientation of the radiation terminal, an independent characterization must be made, which gives rise to a new different set of gauges like correlation, diversity gains etc. The latter has created a trend for engineers to seek a reference environment. Indeed, for a viewer on the coordinates of the terminal, the AoA distribution for different orientations of it could *in average* be represented by a uniform function.

Furthermore, concerning polarization of the incoming EM waves, since a mobile terminal can have any arbitrary orientation in space, the same kind of reasoning given for AoA can be applied equally well here too. Hence, the notion of balanced polarization has been coined to indicate incoming EM waves of arbitrary polarizations. The last two features, i.e., uniform distribution of AoA and balanced polarization, establish the main characteristics of a type of reference environment referred to as *isotropic* environment. This particular environment achieves a practical appeal mostly due to the fact that it can be almost precisely emulated in a fine reverberation chamber [9].

To address the curiosity about the nature of the incoming EM waves e.g., distribution

[4] Consideration of non-uniform AoA is not within the research framework defined for the current thesis.

of their amplitudes and phases, we refer to many experimental results in which it has been shown that amplitude of the received voltages at the ports of the elements comply with Rayleigh distribution [10, sec.1.1]. Since, the voltages could be considered as a weighted sum of the incident electric fields upon the antenna, based on the central limit theorem [11], the incident electric fields could presumably be random variables of independent, identical distribution regardless of the precise forms of their distribution functions. Hence, for the sake of convenience and for empirical reasons alone, zero mean complex Gaussian random variable stands a brilliant model to be used for these incoming EM waves. For instance, electric field of an arbitrary polarized incoming wave from a solid angle direction of Ω can be given by

$$\vec{E}(\Omega) = E_\theta(\Omega)\hat{\theta} + E_\psi(\Omega)\hat{\psi} \quad (\mathrm{V/m}) \ , \tag{1.1}$$

wherein E_θ and E_ϕ are independent complex Gaussian random variables.

1.3 Summary

The current short chapter was devoted to some background about usage of multi-port antennas in multipath environments. A few privileges rendered by them were listed and explained. Some discussion was made for comparison between the conventional and contemporary characterization of antennas. It was emphasized that the role of the shape of the patterns of antennas had been weakened for those designed to work in fading environments. Some words were dedicated to the characteristics of incoming EM waves in multipath environments and the way they are modeled.

Chapter 2

Performance Parameters

The multidisciplinary nature of wireless communication systems results in different interpretations and inferences of the similar concepts leading, in turn, to inconsistent nomenclature among different research groups worldwide. Therefore, before entering to the heart of our analysis, we shall dedicate adequate time to clarify certain terms to be used later on. In light of the clarifications to be made in this chapter, the subsequent parts of the thesis are understood more fluently. The first section deals with the definition of different diversity gains and some interesting and noteworthy points about them. The second section is dedicated to definitions of different correlations and throws light upon their relations in a consistent way. Last but not least, the third section is reserved for efficiency characterization of multi-port radiation systems. There is much evidence in the literature amplifying the role of radiation efficiencies in ultimate performance of the multi-element antennas. In this regard, the latter section requires more attention and merits further dedications. As a point of caution, we reiterate that *isotropic environment* to be used in this chapter is referred to multipath environments of uniform AoA and balanced polarization. Note that, some elucidations concerning different capacities and the way they are evaluated in the frame of our work are set aside and deferred to section 4.2 on page 30. Therefore, capacity is not addressed in this chapter.

2.1 Diversity Gain

Despite the fact the diversity gain bears a key-role in evaluation of MIMO systems designs, it lacks a unanimous definition among researchers worldwide. While communication engineers have their own interpretation of the gains rendered by multiple element antennas' usage [1]-[14], the antenna experts look upon multi-port terminals differently [15]-[18]. Hence, the main concern of this section is to clear out what we refer to as diversity gain throughout this report. Then, some words are to be said regarding different prevalent schemes chosen for achieving diversity gains and the upper bounds that are affiliated with them.

2.1.1 Definition

Wireless communication links are exposed to fluctuations in the signal level in time, frequency and space domain, referred to as fading. That is, there is a finite probability for each signal to frequently undergo a certain threshold level resulting in loss of connection. To mitigate the problem, the choice of using multiple element antennas, say diversity branches, have been introduced. Increasing the number of diversity branches, indeed, reduces the chance of simultaneous fading over all of them. Therefore, by virtue of some simple combining techniques, the possibility of loosing connection in a multipath environment can be reduced considerably. Note that combining can be realized in several ways having different level of complexity [12]. Some renowned combining techniques are selection combining, switched combining, Equal Gain Combining, and maximum-ratio combining [12].

In the frame of this thesis, among different mentioned combining schemes, we concentrate on maximum ratio combining (MRC) and selection combining (SC) ones. The former is chosen for its bestowing an optimum performance whereas the latter is more known for its simplicity[1]. In the MRC scheme, the signal is firstly co-phased and then the combiner outputs a weighted sum of the signals available at all ports yielding maximum possible SNR at the receiver. On the contrary, in the SC scheme, the combiner outputs the signal at the port with highest power. Both mentioned schemes have been elaborated in depth in different literatures[2] and the interested reader is referred to them.

Diversity gain, though has its real meaning inherent in its name, can be interpreted from different standpoints. From communication system point of view, diversity gain is the slope of the bit error rate versus Signal to Noise Ratio (SNR) curves of logarithmic scales in both axes. Naturally this slope is considered for the linear part of the curves, which corresponds to relatively larger SNRs. In this way, the diversity gain is dependent on different parameters such as the detection method and the type of the modulation [1]-[14]. To conquer this issue, engineers restrict themselves to a certain modulation scheme e.g., BPSK, and use the symbol error rate (SER) curves instead of BER ones [1]. Also, bear in mind that to focus on the study of diversity gain, communication engineers consider repetition coding through different branches which incurs a reduced spectral efficiency [1].

The discussion presented above is rather formal and involved. From antenna point of view, things are a bit less obvious when we incorporate many system parameters involved for definition of diversity gain. This fact leaves no room for antenna engineers unless an alternative definition and interpretation of the diversity gain. Therefore, different diversity gains have been defined based on the received signals cumulative distribution function (CDF) curves, measured in a fading environment. In this way, *apparent diversity gain* (ADG) is defined as the ratio between the strength of the diversity signal and the best branch's one at %1 level of their CDF curves. In other words, if the CDFs are drawn in logarithmic format, the difference between the CDF curve of the diversity signal achieved from certain combining scheme and the best branch's one forms the ADG. Furthermore, *effective diversity gain* (EDG) is defined as the ratio between the strength of the diversity signal and an *ideal* reference antenna's one, measured in ideally the same environment, at %1 level of their CDF curves. By *ideal* we mean an antenna with unit radiation efficiency.

[1] Note that it is not the simplest one regarding the implementation.

[2] For instance, look at [10, Chap. 5] or [12, Chap. 7].

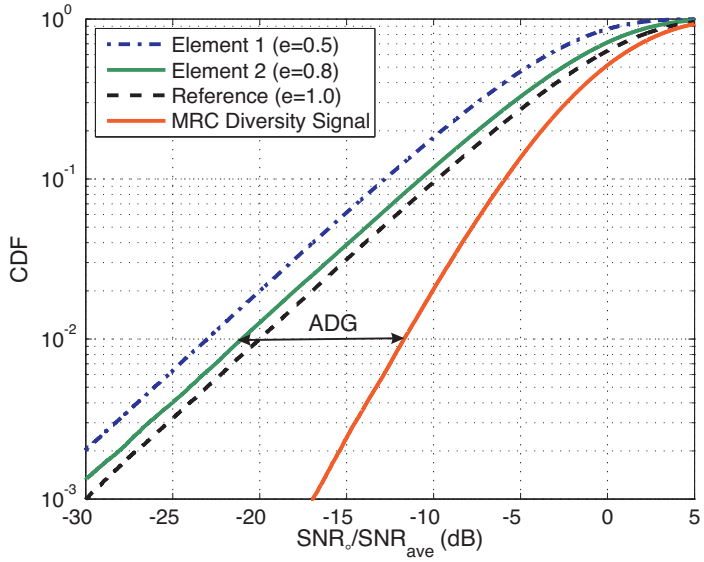

Figure 2.1: Definition of ADG for an arbitrary two-port antenna in an isotropic environment. The envelope correlation between the two elements is $\rho^{\mathrm{e}} = 0.5$.

In a rich isotropic environment, as long as a single-port ideal reference antenna is used, the relation between the aforementioned diversity gains become:

$$\mathrm{EDG} = e_{\mathrm{tot}_{\max}} \cdot \mathrm{ADG} \ , \tag{2.1}$$

where $e_{\mathrm{tot}_{\max}}$ is the total embedded radiation efficiency of the best branch. Indeed, EDG renders a possibility to find out how well our diversity radiation system performs in comparison with a single ideal isotropic antenna. It shall be clear that in case of a non-uniform multipath environment, the total embedded efficiency in (2.1) should be replaced by *mean effective gain* [3]. Fig. 2.1 illustrates the definition of ADG for an arbitrary two-port antennas in a Rayleigh fading isotropic environment. EDG can simply be envisioned as the distance between the dashed curve and the MRC diversity curves. The *envelope correlation*[3] between the signals available at these ports is $\rho^{\mathrm{e}} = 0.5$.

Now that the definitions of ADG and EDG have been cleared, the first question that emerges is as in a Rayleigh fading environment ultimately how much ADGs can be achieved by using different number of elements in our radiation terminal. This question will be addressed in the following short section.

2.1.2 Maximum Possible Diversity Gain

It is a matter of concern as ideally how much diversity gain we can achieve in uncorrelated Rayleigh multipath environments. In a general Rayleigh fading environment i.e., arbitrary AoA distribution, the maximum possible ADG occurs for multi-port antennas with similar average received power at their ports and no correlation between their received signals. In contrast, in a rich isotropic environment, the maximum EDG happens for the case in which both elements have no correlation and are of unit embedded element radiation

[3] It is defined in (2.6) on page 12.

Table 2.1: Maximum achievable ADG for SC and MRC Schemes.

	$\mathrm{ADG_{max}}$ dB	
No. of Elements	SC scheme	MRC scheme
1	0.0	0.0
2	10.2	11.7
3	13.8	16.4
4	15.8	19.1
5	17.0	21.0
6	17.9	22.5
7	18.6	23.7

efficiencies. Under this constraint, both ADG and EDG present the same maximum limit. Hence, we focus on the rich isotropic environments and restrict ourselves to them. For this purpose, we ought to theoretically find the CDFs of the combined signals. For instance, let us opt for SC scheme. Based on the definition of SC scheme, for an M-branch multi-element antenna, the CDF ($\mathbf{P}_{\mathrm{SC}}$) can be set by its probability density function (PDF), $\mathbf{p}$, as in [10],[12]. Naturally, when the maximum of a group of numbers is less than a particular amount, it necessitates that all of them be simultaneously less than it[4],

$$\mathbf{P}_{\mathrm{SC}}(r) = \mathbf{p}(r_{\mathrm{SC}} < r) = \mathbf{p}(\max[r_1, r_2, \ldots, r_{\mathrm{M}}] < r) \ . \tag{2.2}$$

On the other hand, by assuming no dependancy between the variables, meaning that they are uncorrelated, (2.2) becomes

$$\mathbf{P}_{\mathrm{SC}}(r) = \prod_{m=1}^{\mathrm{M}} \mathbf{p}(r_m < r) \ , \tag{2.3}$$

where, $\mathbf{p}$ stands for the PDF of the corresponding received signal. By assumption of Rayleigh distributed received signal, $\mathbf{P}_{\mathrm{SC}}$ in (2.3) can be found. Later, by a numerical method the argument $r_\circ$, at which $\mathbf{P}_{\mathrm{SC}}$ reaches its 1% level, can be obtained. Now, having $r_\circ$ in access, we can readily calculate the corresponding maximum ADG. In a tantamount way, a closed-form formula for MRC case can be also achieved and solved numerically to give the corresponding maximum ADG [10].

Based on the discussion presented above, the results of our calculation up to M = 7 number of ports are summarized in Table 2.1. Note that the more the number of diversity branches, the less the sequential enhancements in the corresponding achievable diversity gain. For instance, by SC diversity scheme, the increase in diversity gain from two branches to three branches is 3.6 dB; whereas, from M = 19 to M = 20 is only 0.4 dB.

2.1.3 Measurement of ADG

The main concern regarding the definition of ADGs at 1% level of received signals' CDF curves is its accurate measurement. In a fading environment due to the statistical nature of

[4] This fact reminds the AND operator.

the signals at different ports of a multi-element antenna, unless an adequate and normally huge number of measured samples of the received signals are available, the corresponding CDF curves deviate from their converged counterparts down at 1% level. For instance, based on the results in [19, Table 1], in order to reach an accuracy better than 0.25 dB the number of independent measured samples should exceed ten thousands.

Collecting an enormous number of measured samples at ports of a multi-element antenna in a multipath environment is unacceptably cumbersome, if not impossible. Also, reverberation chambers, which are presently prevalent for diversity gain measurements in isotropic environments, are limited to a finite number of independent samples. Indeed, reference [19] introduces one way to come over this problem for a case of two-port antennas. Yet, the approach upon which the paper evolves can be used to bypass this difficulty. Last words, it is important to note that the current difficulty will be pronounced more for radiation systems with higher number of ports.

2.2 Correlation

In multi-element antenna system, *correlation* between any two different elements refers to the correlation between the received signals of the corresponding branches [8]. Indeed, it is a measure of similarities between two different ports' signals. In MIMO communication systems, the maximum capacity of the system cannot be achieved unless the correlation between different elements is zero. This fact renders an impressive role to the mentioned parameter, which necessitates a better regard. There are few factors effective on this entity. They are AoA distribution[5], and embedded element far field functions. In the literature, some factors like mutual coupling and spatial structure have been considered also as efficacious in correlation [8]. However, both of the foregoing factors are inherent in embedded far field functions of the elements. Therefore, we avoid treating them individually though acknowledging that their influence can be also studied separately.

Furthermore, it is important to note that spatial correlation affects the slope of the CDF curve of diversity combined signal and the efficiency gives some shifts to signals' CDFs. That how much efficiency shifts the diversity signals' CDF curve is a question of interest and at least for cases of a two-port antenna has been shown in [19]. To mathematically formulate the correlation, let us first presume two voltage vectors, $\bar{V}_i$ and $\bar{V}_j$, measured at ith port and jth port of a multi-element terminal in a fading environment. The entries of these two vectors can be envisioned as measured voltage samples at the corresponding ports in different scenarios. The *covariance*, $\mathbb{C}$, defined upon these two vectors are calculated by

$$\mathbb{C}(\bar{V}_i, \bar{V}_j) = \mathbb{E}\left((\bar{V}_i - \mathbb{E}(\bar{V}_i))(\bar{V}_j - \mathbb{E}(\bar{V}_j))^{\mathrm{T}}\right) \ . \tag{2.4}$$

where $\mathbb{E}$ indicates the expectation operator and $.^{\mathrm{T}}$ stands for transpose. Now, the correlation coefficient, known as *complex correlation* between the branches i and j, is given

[5] A further parameter called *cross polarization coupling* is also influential which is beyond the scope of the current report being restricted to balanced polarization.

by:[6]

$$\rho_{ij} = \frac{\mathbb{C}(\bar{V}_i, \bar{V}_j)}{\sqrt{\mathbb{C}(\bar{V}_i, \bar{V}_i) \cdot \mathbb{C}(\bar{V}_j, \bar{V}_j)}} \,. \tag{2.5}$$

Normally, the phase of the complex correlation is insignificant in comparison with its amplitude. Therefore, the absolute value of complex correlation is mostly regarded and simply referred to as *correlation*. Thus, from now on, whenever we refer to correlation, we mean $|\rho|$ defined in (2.5).

In addition to this, measurements of the voltage sample as a complex vector with an amplitude and a phase seem more troublesome than the associated time average power samples.[7] Therefore, in cases where the power sample vectors are in access, *envelope correlation*, ρ^{e}, is used. Should we denote the associated power vectors at port i and j by $\bar{P}_i$ and $\bar{P}_j$, respectively, the envelope correlation is then

$$\rho^{\mathrm{e}}_{ij} = \frac{\mathbb{C}(\bar{P}_i, \bar{P}_j)}{\sqrt{\mathbb{C}(\bar{P}_i, \bar{P}_i) \cdot \mathbb{C}(\bar{P}_j, \bar{P}_j)}} \approx |\rho_{ij}|^2, \tag{2.6}$$

with the corresponding covariance operator defined similar to (2.4). In [10], it is said that the envelope correlation approximates the squared correlation, which is reflected in (2.6). In [20, Fig.1], it is shown that the relative error in this approximation does not exceed 3%.

We stress that under certain ideal circumstances -which is not far from reality- both correlation and envelope correlations can be achieved from *embedded element far field functions* of the corresponding branches. The latter requires a discipline of its own[8]; yet, for the time being, it suffices to say that the embedded element far field function of an element, $\vec{G}_{\mathrm{emb}}$, is the far field function measured or simulated when the corresponding element is excited by the pertinent source at its port whereas all other present ports are terminated to their own terminating impedances. Having said that, we directly present the formula for e.g., envelope correlation, as follows

$$\rho^{\mathrm{e}}_{ij} = \frac{\left| \oint_{4\pi} \vec{G}_{\mathrm{emb}_i} \cdot \vec{G}^{*}_{\mathrm{emb}_j} d\Omega \right|^2}{\oint_{4\pi} |\vec{G}_{\mathrm{emb}_i}|^2 d\Omega \cdot \oint_{4\pi} |\vec{G}_{\mathrm{emb}_j}|^2 d\Omega} \,. \tag{2.7}$$

Now, let us spend a few moments to clarify some noteworthy points about the features of the aforementioned environment wherein (2.7) holds. First and foremost, this multipath environment has uniform angle of arrival for the incident EM waves. Moreover, for these incoming waves, it is assumed that both polarizations are uncorrelated and equally likely. In addition to this, they have the same average power density i.e., balanced polarization. To clarify the former point, we stress that at each incident direction, orthogonal polarizations are uncorrelated. Furthermore, the incoming waves of the same polarization are

[6] In MATLAB, the command 'corrcoef' uses the same formula as here.

[7] Measurements in a reverberation chamber in which both transmit and receive antennas are connected to the same vector network analyzer is an exception.

[8] Find more about it at section 3.3.1 on page 22.

spatially uncorrelated. Last but not least, it is presumed that the incident EM waves are samples of an ergodic random variable [21]. The keen reader may realize that based on the central limit theorem [11], having numerous independent incident waves upon an antenna results in a Rayleigh distributed received signal at its port. Therefore, in its precise form, equation (2.7) is solely credible in Rayleigh multipath environments of isotropic features and shall not be used for other types of environments. For your consideration, we state that the isotropic environment created in a fine reverberation chamber approximates this ideal multipath environment to a considerable extent. For this reason, the reverberation chambers have been granted a great deal of attention recently.

As the last point, we recall that in general and from mathematical point of view, correlation coefficient, ϱ, resides within the range $-1 \leqslant \varrho \leqslant 1$. However, an interesting feature for the signals of Rayleigh distribution is that the envelope correlation, ρ^{e}, as defined in (2.6), is a non-negative measure [21]. This fact removes any ambiguity concerning the potential conflicts in signs that could possibly obsess the keen readers.

2.3 Efficiency Characterization of Multi-port Antennas

We address a novel way of expressing the radiation characteristics of multi-port antennas which is not only in harmony with the classical concept of radiation efficiencies of a single port antenna, but also of interest for its ease of measurement. Of practical concern is the case in which all present elements are terminated to the characteristic impedance of the system, $Z_\circ$, being normally of pure resistive nature. In this specific case, all efficiency pertinent parameters can be recast in terms of scattering parameters. Thus, we restrict ourselves to this assumption for the following parts. Furthermore, for the sake of simplicity, from now on, we refer to impedance of $Z_\circ$ as *match termination*.

For an antenna element at the presence of other elements, aside from losses in the non-ideal conductors, dielectrics and lossy objects, absorption in terminations of other neighboring elements as well as reflection on its own port contribute to the reduction of its radiation efficiency. *Total embedded element efficiency* of an antenna is, indeed, a measure indicating reduction of radiation performance caused by the aforementioned factors. In what follows we deal with different parameters characterizing these influential factors. But before that, we shall set a few notations.

2.3.1 Some Definitions and Notations

Maximum available power from the source[9], denoted by P_{avs}, is the maximum power available from the source of certain internal impedance, which –for the time being– is assumed to be the same as the characteristic impedance of the system, as mentioned. Moreover, power dissipated in all present match terminations due to coupling through

[9] We will, henceforth, refer to it shortly as *available power*.

excitation at port i is referred to P^i_{cpl} given by

$$P^i_{\text{cpl}} = P_{\text{avs}} \sum_{j=1}^{N} |s_{ji}|^2 , \tag{2.8}$$

wherein N refers to the total number of the ports i.e., elements. As a point of caution, we stress that the reflected power at the port i denoted by P^i_{rfl} is, indeed, included in P^i_{cpl} and is evaluated by

$$P^i_{\text{rfl}} = P_{\text{avs}} |s_{ii}|^2 . \tag{2.9}$$

Moreover, the *accepted power*, P_{acc}, is defined as that part of the available power which is delivered to the corresponding element for radiation. It should be clear that a portion of the power which is coupled and is dissipated on the terminations of other present ports is not potentially available for radiation; thus, an alternative name for accepted power could be *decoupled power*. Given that the element i is excited, the accepted power associated with it can be calculated by

$$P^i_{\text{acc}} = P_{\text{avs}} - P^i_{\text{cpl}} . \tag{2.10}$$

Bear in mind that the mentioned definition of the accepted power is a general definition. In case of a single radiation element, there will be no coupling, hence the coupled power as defined above becomes equal to the reflected power at its own port.

In addition, in the case of ohmic losses on the elements or at the presence of a lossy object, a portion of the accepted power will be dissipated and is referred to as *loss power*, P_{los}. Now, what is left forms the radiated power which is denoted by P^i_{rad}. That is,

$$P^i_{\text{rad}} = P^i_{\text{acc}} - P^i_{\text{los}} , \tag{2.11}$$

where P^i_{los} stands for losses over the radiation structure when element i is excited and all other elements are match terminated. Having set those, now we have all the necessary ingredients in access to define different useful parameters.

2.3.2 Embedded Element Efficiencies

By definition, in a multi-element antenna system, *embedded element efficiency* of element i, e^i_{emb}, is the ratio between the radiated power and the accepted power while port i is excited and all other present ports are match terminated,

$$e^i_{\text{emb}} = \frac{P^i_{\text{rad}}}{P^i_{\text{acc}}} . \tag{2.12}$$

In the same way, *total embedded element efficiency* for port i, e^i_{tot}, is the ratio between the radiated power and the available power,

$$e^i_{\text{tot}} = \frac{P^i_{\text{rad}}}{P_{\text{avs}}} . \tag{2.13}$$

2.3.3 Decoupling Efficiency

Based on what has been mentioned, the less the coupling among the neighboring elements, the higher the accepted power. In an ideal case of no ohmic losses and no coupling, all input power to the element then radiates from it. Indeed, this fact has created a trend among engineers to reduce the coupling as much as possible in order to enhance the elements' performances. To measure engineers' success in this respect, a parameter has been coined which can best be called *decoupling efficiency* [22]. Decoupling efficiency, e^i_{dec}, is defined as the ratio between the accepted power by excitation at port i and the incident power at this port.[10]

$$e^i_{\text{dec}} = \frac{P^i_{\text{acc}}}{P_{\text{inc}}} = 1 - \sum_{j=1}^{N} |s_{ji}|^2 \tag{2.14}$$

Note that associated with each port, there comes a certain decoupling efficiency specified by (2.14). Considering (2.13), (2.12) and (2.14), the total embedded efficiency can be recast as

$$e^i_{\text{tot}} = e^i_{\text{emb}} \cdot e^i_{\text{dec}} \ , \tag{2.15}$$

which reminds the classic definition of total radiation efficiency of a single-port antenna ($e_{\text{tot}} = e_{\text{mch}} \cdot e_{\text{rad}}$) in which *matching efficiency*, e_{mch}, is defined as follows:

$$e_{\text{mch}} = \frac{P_{\text{acc}}}{P_{\text{avs}}} = 1 - |\Gamma|^2 \ , \tag{2.16}$$

with Γ being the reflection coefficient at the port. There are few points concerning decoupling efficiency worth noting. The first point is that based on the definition given, the decoupling efficiency is assessed by means of scattering parameters of the system which are not relatively difficult to measure. If we had defined it based on radiated power, it would have required a thorough measurement of radiated power, which is a tedious task. Moreover, a salient feature of decoupling efficiency is that in many practical cases it would stand as a fine indicator of total embedded efficiency. In fact, with the one proviso that there be no power dissipation on the structure i.e., $e_{\text{emb}} = 0$ dB, the decoupling efficiency becomes the same as total embedded efficiency of the corresponding element.[11] Furthermore, as a final point, bear in mind that the definition of decoupling efficiency is a general one, which in case of a single element or alternatively no coupling among the elements of a multi-element radiation terminal reduces to the classic matching efficiency. Hence, the latter might be considered as a special case of the former.

2.4 Summary

This chapter was dedicated to some important parameters in characterization of multi-port antenna systems in multipath environments. The chapter threw light upon diversity gain's definition used by antenna engineers and outlined some significant points concerning

[10] Note that here we have restricted ourselves to match terminated ports. Thus, the incident power at the port equals the maximum available power from the source e.g., $P_{\text{avs}} = P_{\text{inc}}$.

[11] Recall that we are only concerned about match terminations.

this critical parameter. Later, a fairly detailed section was spent on different correlations and the ways whereby they are evaluated. In the last part of the chapter, a novel and unified way of expressing the efficiency performances of multi-port radiation terminals was introduced. The notion of decoupling efficiency, which has been in use quite recently, was addressed to some extent in this part.

Chapter 3

Formulation of the Received Signals

The main concern of the current chapter is to derive some useful formulas rendering the received voltage and the associated power signals at the port(s) of an antenna system upon presumption of a known incident EM wave. The formulas will be precisely derived and the steps in their derivation are elaborated to a point of satisfaction while details remain within our patience. The derivation has been established based on the previous work in the department [15]. However, it gives a more general appearance to the previously achieved formulas in a sense that it includes the non-ideal radiation efficiencies into account. In addition to that, since the approach upon which the formulations have been evolved is independent from the previous counterpart work, the normalizations used in them are different. We stress that the current expressions present a consistent normalization and are credible in general circumstances. Therefore, the current developments are, by no means, a repetition of the previously published material and merit some more time and dedications. The chapter starts with the simple case of single-port antenna terminated to the characteristic impedance of the system. Then, it is generalized to a case in which the antenna has an arbitrary impedance at its port. The latter will then be generalized to a case in which we have a multi-port antenna system with inherent coupling between its ports. The concept of embedded element far field function is then clarified and the way it is evaluated is cleared. The chapter will be closed by virtue of a verification study in which the power formulation achieved will be shown to be in consistent with the previously published results.

3.1 Case of Matched Terminated Single-port Antenna

Before entering to the heart of our derivation we need to recall a few points. First of all, it is supposed that the antenna's far field function is measured or excited by a source of $Z_\circ$ internal impedance. It is also assumed that the presumed antenna, to be used in receive mode, is connected to a receiver of the $Z_\circ$ impedance. Hence, due to reciprocity the properties of this antenna in receive mode and transmit mode are similar. We start with formulation of the received average power and later pursue our development to the voltage vector.

3.1.1 Formulation of Power Signal

The maximum power that can be received by the termination of our antenna is given by

$$P_{\max} = \frac{|V_r|^2}{8R_{\text{ant}}} \tag{3.1}$$

wherein V_r is the available induced voltage at the open circuited port of our antenna. It happens in cases where we have a conjugate matched termination, i.e. $Z_{\text{ant}} = R_{\text{ant}} + jX_{\text{ant}} = {Z_{\text{L}}}^*$.[1] However, in our case where the antenna is terminated by $Z_\circ$ (matched terminated), the received power at the receiver takes the appearance of (3.2) [15],

$$P_{\text{L}} = e_{\text{mch}} \frac{|V_r|^2}{8\Re[Z_{\text{ant}}]} \tag{3.2}$$

where e_{mch} was already defined in (2.16) on page 15 [2] and $\Re$ stands for *real* operator. On the other hand, the radiated power from the antenna is given by [3]

$$P_{\text{rad}} = \frac{1}{2}\Re[Z_{\text{ant}}]|I|^2 \; e_{\text{rad}} \; ,$$

resulting in,

$$|I| = \sqrt{\frac{2P_{\text{rad}}}{e_{\text{rad}} \; \Re[Z_{\text{ant}}]}} \; . \tag{3.3}$$

The left term in (3.3) is the absolute value of the current flowing over the antenna in transmit mode, rendering the radiated power of amount P_{rad}. A formula for the received voltage upon a known incident EM wave is provided in [24], in which η is the intrinsic impedance of the medium [25, pp 363], and λ is the pertinent wavelength. As a reminder, $\vec{G}_r$ is the far field function of the antenna and V_r is the open circuit voltage upon an incident EM wave, $\vec{E}_{\text{inc}}$.

$$V_r = \frac{-2j\lambda}{\eta \; I} \vec{G}_r \cdot \vec{E}_{\text{inc}} \tag{3.4}$$

Substituting (3.3) and (3.4) in (3.2) yields

$$\sqrt{P_{\text{L}}} = \left| \frac{-2j\lambda}{\eta} \sqrt{\frac{e_{\text{rad}}\Re[Z_{\text{ant}}]}{2P_{\text{rad}}}} \sqrt{\frac{e_{\text{mch}}}{8 \; \Re[Z_{\text{ant}}]}} \vec{G}_r \cdot \vec{E}_{\text{inc}} \right| \; ,$$

leading to

$$P_{\text{L}} = \left| \frac{-j\lambda}{2\eta} \sqrt{\frac{1}{P_{\text{avs}}}} \vec{G}_r \cdot \vec{E}_{\text{inc}} \right|^2 \; . \tag{3.5}$$

The above equation can be simplified by dragging the constant terms out of the squared absolute value to give it some more appealing appearance.

$$\boxed{P_{\text{L}} = \frac{\lambda^2}{4\eta^2 \; P_{\text{avs}}} \left| \vec{G}(\Omega_k) \cdot \vec{E}_{\text{inc}}(\Omega_k) \right|^2} \tag{3.6}$$

[1] Note that $R_{\text{ant}} = R_{\text{rad}} + R_{\text{los}}$ where R_{los} represents the conduction-dielectric losses [23, pp. 78].
[2] In this problem, $\Gamma = \frac{Z_\circ - Z_{\text{ant}}}{Z_\circ + Z_{\text{ant}}}$.
[3] The radiation efficiency, e_{rad}, used here is equivalent to e_{emb} in case of a single-port antenna.

It is crucial to note that the above formula is solely valid under matched termination constraint. Recall that the term P_{avs} is the available power from the source ($Z_s = Z_\circ$) whereby the far field function in (3.6) is either measured or simulated. Moreover, the given formula shows that the maximum received power by any antenna depends upon the far field function as well as the available power by which the far field function is measured. It also depends on the strength of the incoming wave, $\vec{E}_{\text{inc}}$, whose unit is volts/meter/steradian.

3.1.2 Formulation of Voltage Signal

In the preceding section, we have dealt with the associated received power at the port of a single element matched terminated antenna. Indeed, this issue has been the target of some other literature wherein different formulas were presented for the same purpose (e.g., have a glance at [26, Chap.5], [23, eq. 2-112] or [21, eq. 81]).

To deal with the received voltage signal at $Z_\circ$ termination of our single port antenna, we take advantage of the vector effective length of the antennas introduced in (3.4) [24]. If we presumably take the phase of the current by which the far field function is measured or simulated equal to zero (i.e., it is considered as our phase reference), then the actual value of the current in (3.3) becomes the same as its absolute value. Therefore, we can write

$$\begin{aligned} V_r &= \frac{-2j\lambda}{\eta\sqrt{\frac{2P_{\text{rad}}}{e_{\text{rad}}\cdot\Re[Z_{\text{ant}}]}}}\vec{G}_r \cdot \vec{E}_{\text{inc}} \\ &= \frac{-2j\lambda}{\eta}\sqrt{\frac{\Re[Z_{\text{ant}}]}{2P_{\text{acc}}}}\vec{G}_r \cdot \vec{E}_{\text{inc}} \end{aligned} \tag{3.7}$$

Now, using the equivalent circuit in [23, Fig. 2.21], the received voltage appearing at $Z_\circ$ impedance connected to the port becomes

$$\boxed{V_{\text{L}} = \frac{-2j\lambda}{\eta}\sqrt{\frac{\Re[Z_{\text{ant}}]}{2P_{\text{acc}}}}\frac{Z_\circ}{Z_{\text{ant}}+Z_\circ}\,\vec{G}_r(\Omega_k)\cdot\vec{E}_{\text{inc}}(\Omega_k)}\,. \tag{3.8}$$

Equation (3.8) is of particular concern serving our purpose better since it plays a central role in capacity calculation of the channel, which is based on the channel matrix[4]. One may verify the consistency of (3.6) and (3.8) by virtue of

$$P_{\text{L}} = \frac{1}{2\ Z_\circ}\left|V_{\text{L}}\right|^2\ .$$

In the following section, we deal with the formulation of the received signal at the port of a single element antenna with an arbitrary termination.

[4] Refer to Section 4.2 on page 30.

3.2 Case of Arbitrary Terminated Single-port Antenna

This section is divided into two parts. In the first part we study the case in which the impedance connected to the port in measuring the pattern is the same as the desired impedance in receive mode upon which the voltage and power signals are to be formulated. The former impedance, that is the internal impedance of the source by which the antenna's far field function is either measured or simulated e.g., in transmit mode, is denoted by Z_s. In contrast, the latter one, that is the impedance over which the receive mode formulation is going to be established, is referred to as Z_{L}.

3.2.1 Formulation for the case of $Z_s = Z_{\mathrm{L}}$

Up to now we have assumed that the far field function, $\vec{G}_r$, is measured or achieved by a source of internal impedance $Z_\circ$, which is normally of resistive nature.[5] Now, we would like to presume that the source by which the far field function has been measured or simulated has arbitrary complex impedance of Z_s. If the given pattern is going to be used to yield the received power and voltage signals, then the same formulas as (3.6) and (3.8) can be used if and only if the receiver has a complex impedance similar to the corresponding source used in measurement or simulation of the far field function. Yet, we need to inject some points of caution.

First of all, note that the reflection coefficient given in the preceding section has to be modified in order to hold for a general complex impedance [27]. That is,

$$\Gamma = \frac{Z_{\mathrm{ant}} - Z_s^*}{Z_{\mathrm{ant}} + Z_s} \ , \tag{3.9}$$

where the symbol * stands for complex conjugate. The matching efficiency based on the above reflection coefficient can then be evaluated to be

$$e_{\mathrm{mch}} = \frac{4\Re[Z_{\mathrm{ant}}]\Re[Z_s]}{|Z_{\mathrm{ant}} + Z_s|^2} \ . \tag{3.10}$$

Recall that the available power in this case becomes

$$P_{\mathrm{avs}} = \frac{|V_s|^2}{8\ \Re[Z_s]} \ , \tag{3.11}$$

whence the accepted power can be recast as

$$P_{\mathrm{acc}} = e_{\mathrm{mch}} \cdot P_{\mathrm{avs}} \ . \tag{3.12}$$

By substitution of the aforementioned parameters, the received power and voltage signals can be obtained from (3.6) and (3.8).

[5] For instance, $Z_\circ = 50\Omega$.

3.2.2 Formulation for general choices of Z_s and $Z_{\rm L}$

Now, assume that we have measured the far field function by virtue of a source of certain voltage, V_s, as before and an arbitrary complex internal impedance of Z_s. Having this far field function, $\vec{G}_r$, in access, we wish to formulate the voltage and the associated power at arbitrary complex load impedance of $Z_{\rm L}$ created by an arbitrary complex incident electric field of $\vec{E}_{\rm inc}$.

Should we presumably take the far field function proportional to the current flowing over the antenna structure, it can be shown that the preceding formulation for the associated power signal takes the appearance of

$$\boxed{P_{\rm L} = \frac{\lambda^2}{4\eta^2 P_{\rm avs}} \left|\vec{G}_r \cdot \vec{E}_{\rm inc}\right|^2 \cdot \frac{\Re[Z_L]}{\Re[Z_s]} \left|\frac{Z_{\rm ant} + Z_s}{Z_{\rm ant} + Z_{\rm L}}\right|^2} \,. \tag{3.13}$$

We reiterate that $P_{\rm avs}$ is the maximum available power from the source of Z_s internal impedance (3.11). The corresponding voltage at the termination, $Z_{\rm L}$, can then be achieved by

$$\boxed{V_{\rm L} = \frac{-2j\lambda}{\eta} \sqrt{\frac{\Re[Z_{\rm L}]}{2P_{\rm acc}}} \frac{Z_{\rm L}}{Z_{\rm ant} + Z_{\rm L}} (\vec{G}_r \cdot \vec{E}_{\rm inc})} \tag{3.14}$$

where, of course, $P_{\rm acc}$ stands for the accepted power by the antenna when excited by a source of Z_s internal impedance. It is given in (3.12). Again, one may readily show that the power, which is dissipated in $Z_{\rm L}$ by the voltage given in (3.14), is the same as (3.13); that is, both (3.13) and (3.14) read

$$P_{\rm L} = \frac{1}{2}\Re[V_{\rm L} I_{\rm L}^*] \,.$$

Please note that in the derivation of the mentioned formulas, we have assumed a single-port antenna case. It is also assumed that the antenna is small and simple in the sense that the losses over the antenna can be modeled with a loss resistance in series with its radiation resistance. For instance, for antennas over a lossy ground plane or with lossy dielectric, the aforementioned model may not be applied. Hence, they are not considered in these formulations. Yet, as long as the antenna's equivalent circuit including the corresponding losses is known, the same routine used above can be applied in order to bestow the affiliated voltage and power vectors. If the equivalent circuit is not available, the only way left is to re-measure or re-simulate the antenna terminated with the desired complex impedance at its port. In the following section, we shall deal with the more interesting case of multi-port antennas.

3.3 Case of Multi-port Antennas

Before elaborating the derivation of any formulation for the current section, we need to clarify an important point. Indeed, it is of foremost significance to understand that the performance of an element at the presence of other neighboring elements depends not

only on the performance of the antenna itself, but also upon the inevitable coupling which appears in these radiating structures. On the other hand, based on the antenna theory, the performance of any antenna can be analyzed merely through its far field function and the input impedance, not to mention its total radiation efficiency. This fact is, of course, still credible under presumption of some neighboring antenna elements, which are coupled to the pertinent one. In this case, the concept of *embedded element far field function* is used to describe the spatial performance of the associated antenna element. In this way, the total radiation efficiencies give their place to the total embedded element efficiencies elucidated in section 2.3.2 on page 14. Therefore, in the following section, we shall elaborate the concept of embedded element far field function.

3.3.1 Embedded Element Far Field Function

In general, the embedded element far field function associated to the ith antenna element in a multi-port antenna system, denoted by $\vec{G}^{i}_{\text{emb}}$, is referred to the measured or simulated far-field function when the associated source connected to the ith port[6] is switched on whereas all other sources with arbitrary internal complex impedances connected to them are turned off. There are three categories of embedded far field functions being of particular interest. The first group of them are the embedded far field functions of the elements while all present elements are terminated to the characteristic impedance of the system, $Z_\circ$, which, like before, is of resistive nature e.g., $Z_\circ = 50\Omega$. Let us refer to these embedded far field functions as the *matched embedded far field function*. These far field functions come in picture more in practical circumstances, for instance, in the reverberation chamber measurements. In addition to them, the *short-circuit embedded far field function* refers to the embedded far field function when the corresponding element is excited while all other elements are short-circuited. In a tantamount way, we can define the *open-circuit embedded far field function* affiliated to the case where, except the excited port, all other present ports are open-circuited.

This section is partitioned in two subsections. The difference between these two sections is associated with the set of impedances connected to the ports in measuring the antennas and in using them as the receiver. In the first part we study the case in which the sets of impedances connected to the ports are the same. In the second part, we deal with the general cases in which the two mentioned sets of impedances are different. For convenience in notation, let us recast the set of the impedances connected to different ports in measurement or simulation phase in a matrix-form and denote it by $\bar{\bar{Z}}_s$. We arbitrarily call it the *source impedance matrix*, which is a diagonal matrix whose entries are the complex impedances connected to the corresponding ports. Thus, for an N-port antenna system, the source impedance matrix can be written as

$$\bar{\bar{Z}}_s \triangleq \begin{bmatrix} Z_{s_1} & 0 & \cdots & 0 \\ 0 & Z_{s_2} & \cdots & 0 \\ \vdots & \vdots & \ddots & \vdots \\ 0 & 0 & \cdots & Z_{s_N} \end{bmatrix}_{N\times N}$$

In the same way, we can also stack the set of the terminating impedances in a matrix called

[6] That is, the port of the ith element.

terminating impedance matrix, $\bar{\bar{Z}}_{\mathrm{L}}$. The entries of the terminating impedance matrix are the associated impedances connected to the ports in receive mode.

$$\bar{\bar{Z}}_{\mathrm{L}} \triangleq \begin{bmatrix} Z_{\mathrm{L}_1} & 0 & \cdots & 0 \\ 0 & Z_{\mathrm{L}_2} & \cdots & 0 \\ \vdots & \vdots & \ddots & \vdots \\ 0 & 0 & \cdots & Z_{\mathrm{L}_N} \end{bmatrix}_{N\times N}$$

3.3.2 Formulation for the case of $\bar{\bar{Z}}_s = \bar{\bar{Z}}_{\mathrm{L}}$

This case is the simplest one, in which quite similar formulas as in (3.6) and (3.8) hold except that the different parameters in them shall be replaced by the corresponding embedded ones. For instance, upon presumption of an incident EM wave from a solid angle direction of Ω_k, the received power at the port i can be recast as

$$\boxed{P_{\mathrm{L}}^i = \frac{\lambda^2}{4\eta^2\ P_{\mathrm{avs}}^i} \left| \vec{G}_{\mathrm{emb}}^i(\Omega_k) \cdot \vec{E}_{\mathrm{inc}}(\Omega_k) \right|^2} \tag{3.15}$$

in which P_{avs}^i is the available power from the source connected to this port by which $\vec{G}_{\mathrm{emb}}$ is achieved. Furthermore, if the current at port i when measuring $\vec{G}_{\mathrm{emb}}^i$ (i.e., I^i) is in access, the received voltage signal can be attained by

$$\boxed{V_{\mathrm{L}}^i = \frac{-2j\lambda}{\eta\ I^i} \frac{Z_{s_i}}{Z_{\mathrm{in}}^i + Z_{s_i}}\ \vec{G}_{\mathrm{emb}}^i(\Omega_k) \cdot \vec{E}_{\mathrm{inc}}(\Omega_k)} \tag{3.16}$$

where Z_{in}^i is the embedded input impedance of the ith port. Note that (3.16) could be also recast in the same way as in (3.8) based on the embedded accepted power.

3.3.3 Formulation for general choices of $\bar{\bar{Z}}_s$ and $\bar{\bar{Z}}_{\mathrm{L}}$

It is hardly desirable to restrict ourselves to certain sets of receivers for a simple reason that in case any single of them has a different impedance, all the embedded patterns shall be re-measured or re-simulated. The latter is cumbersome and needs a proper treatment. Indeed, the best remedy to alleviate the burden of computation is to perform a particular set of measurements or full wave simulations (e.g., open circuits, short circuits etc.) to achieve the open circuit embedded pattern associated to each branch. Later, by virtue of the equivalent circuits based on Z-matrix [7] of the structure and solving for the currents at the ports with arbitrary terminating impedances, we are able to evaluate the embedded element pattern of each element associated to certain set of terminating impedances. To briefly yet sufficiently detail the procedure, let us consider an example.

An equivalent circuit of an arbitrarily terminated two-port antenna system is illustrated in Fig. 3.1 similar to the one used in [16]. We presume that the Z-matrix of the network together with the voltages of the sources by which the two embedded element far

[7] The current approach is used in [16] and [28].

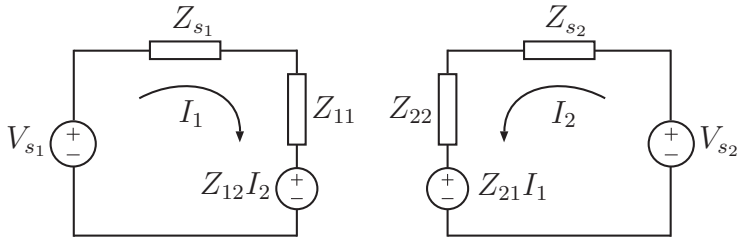

Figure 3.1: Equivalent Circuit of a Two-element Antenna connected to arbitrary sources at its ports.

field functions were measured are available. Also known are the source impedances. The ports' current matrix is thus given by

$$\bar{\bar{I}}_s = (\bar{\bar{Z}} + \bar{\bar{Z}}_s)^{-1} \cdot \bar{\bar{V}}_s \ , \tag{3.17}$$

in which the $\bar{\bar{V}}_s$ is a 2×2 diagonal matrix with V_{s_1} and V_{s_2} shown in Fig. 3.1 as its entries. The open-circuit embedded far field functions of the structure can then be obtained by

$$\bar{\vec{G}}_{\text{oc}} = \bar{\bar{I}}_s^{\,-1} \cdot \bar{\vec{G}}^s_{\text{emb}} \ , \tag{3.18}$$

where, like before, the bar sign upon $\vec{G}$ indicates its being a vector. This vector's two entries are the far field functions of the first and second elements associated to the source impedance matrix[8], respectively. It shall be clear that (3.18) holds at any spatial solid angle, $\Omega(\theta, \psi)$.

Now, if the current antenna system is going to be used in the receive mode with any arbitrary terminating impedances of the receiver, the corresponding embedded far field functions can be achieved as follows. First, the currents at the ports can be obtained through,

$$\bar{\bar{I}}_{\text{L}} = (\bar{\bar{Z}} + \bar{\bar{Z}}_{\text{L}})^{-1} \cdot \bar{\bar{V}}_{\text{L}} \ , \tag{3.19}$$

wherein we arbitrarily choose an identity matrix for the diagonal matrix of $\bar{\bar{V}}_{\text{L}}$. Afterward, the desired embedded far field functions associated with $\bar{\bar{Z}}_{\text{L}}$ are evaluated by means of

$$\bar{\vec{G}}^{\text{L}}_{\text{emb}} = \bar{\bar{I}}_{\text{L}} \cdot \bar{\vec{G}}_{\text{oc}} \ . \tag{3.20}$$

Having achieved that, we have all ingredients (e.g., $\bar{\bar{I}}_{\text{L}}$, $\bar{P}_{\text{avs}}$, and $\bar{\vec{G}}_{\text{emb}}$) in access to calculate the voltage and power signals upon an incident EM wave. They only need to be substituted for the corresponding terms in (3.15) and (3.16). The equivalent circuit of any arbitrary terminated multi-element antennas can be simply envisioned and is already shown in [21, Fig. 6]. We will close the current chapter by deriving the effective area of an antenna based on our formulations, which is the goal of the next section.

3.4 Effective Area of an Antenna

In this section we wish to derive the effective area of an element based on the formulation developed in the preceding sections. In this way, we find also an opportunity to verify our

[8] The superscript $.^s$ indicates that the far field functions are associated with $\bar{\bar{Z}}_s$ terminating impedances.

formulation by some instructive comparisons with other materials published on the same subject on fundamentally different bases.

Effective area or cross section of any antenna was defined under *matched termination* and *polarization* conditions. By those postulations, our derived formula for received power in (3.6), for an incident EM wave can be simply recast as

$$P_{\mathrm{L}} = \frac{\lambda^2}{4\eta^2\ P_{\mathrm{avs}}} |\vec{G}_r(\Omega_k)|^2 |\vec{E}_{\mathrm{inc}}(\Omega_k)|^2, \tag{3.21}$$

Recall that $\vec{G}_r$ is subject to

$$\frac{1}{2\eta} \oint_{4\pi} |\vec{G}_r|^2 d\Omega = P_{\mathrm{rad}}\ . \tag{3.22}$$

Should we denote the embedded power gain far field function of the corresponding element by $\vec{\mathbf{G}}$, then it is subject to

$$\frac{1}{4\pi} \oint_{4\pi} |\vec{\mathbf{G}}| d\Omega = e_{\mathrm{tot}}\ .$$

The power gain pattern was used by R. Collin in [26] whereas we used the square of far field pattern denoted by $\vec{G}_r$ in our formulations. Inasmuch as the spatial configurations of these two parameters are the same, only a normalization factor shall stand for their difference. Therefore, this proportionality coefficient can be simply found to be

$$\vec{\mathbf{G}} = \frac{4\pi}{2\eta} \frac{1}{P_{\mathrm{avs}}} |\vec{G}_r|^2. \tag{3.23}$$

By substituting (3.23) in (3.21), the received power can be rewritten as

$$P_{\mathrm{L}} = \frac{\lambda^2}{2\eta \cdot 4\pi} \mathbf{G}(\vec{\Omega}_k) |\vec{E}_{\mathrm{inc}}(\Omega_k)|^2. \tag{3.24}$$

Furthermore, by virtue of *Poynting* vector as well as postulation of TEM waves for the incoming EM waves, the incident power density associated with $\vec{E}_{\mathrm{inc}}$ becomes

$$P_{\mathrm{inc}} = \frac{1}{2\eta} |\vec{E}_{\mathrm{inc}}|^2. \tag{3.25}$$

When inserted in (3.24), this equality renders

$$P_{\mathrm{L}} = \frac{\lambda^2}{4\pi} \vec{\mathbf{G}}(\Omega_k)\ P_{\mathrm{inc}}\ , \tag{3.26}$$

which is the same as (5.9) in [26]. Now, based on the definition of effective cross section, A_e (i.e., $P_{\mathrm{L}} = A_e \cdot P_{\mathrm{inc}}$), introduced by Collin, within our normalization frame, it can be recast as

$$\boxed{A_e = \frac{\lambda^2}{2\eta P_{\mathrm{avs}}} |\vec{G}_r|^2}\ .$$

The embedded effective area of an element in the presence of other elements can be achieved readily by replacing $\vec{G}_r$ with the corresponding matched embedded element pattern, not to mention the associated P_{avs}. The last point finalizes our chapter.

3.5 Summary

This chapter has been dedicated to a precise formulation of the received voltage and the associated power signal vectors upon a known incident EM wave. First of all, formulations have been made for cases of single-port antennas and later pursued to general cases of multi-element antennas. The formulas were also derived for circumstances wherein the impedance connected to a single-port antenna in the measurement or simulation phase was different from that connected to them in the receive mode. This issue was also considered for a general case of multi-port antenna system. The last part necessitated some elucidations concerning the concept of embedded element far field functions, which was dealt with in this chapter.

Chapter 4

MEST

The current chapter is dedicated to a code called Multipath environment Emulator for performance Simulation of radiation Terminals (MEST) created for characterization of multi-port antennas. Indeed, the software resides on the bases and the theories developed in the preceding chapters. Moreover, the notion upon which the software was established has been introduced and published in [15]. Yet, the formulation and the simulation used there stand for lossless structures. This constraint has been alleviated in the frame of our work, which is elaborated in this thesis. This chapter starts with some elucidation concerning the simulation procedure used in MEST. The inputs and the outputs as well as other necessary parameters are explained carefully. Later, a brief section is dedicated to what we refer to as *Capacity*. The assumptions used in evaluation of the capacity are clarified. Afterward, MEST will be verified by some simulation and measurement results, which are collected in the last section of this chapter.

4.1 Simulation Description

Elaborating the foundations of MEST requires some reminders, which are in order. Please recall that antennas in multipath environments are exposed to several incoming EM plane waves of arbitrary polarization. Each EM plane wave, coming from a certain direction in space known as AoA[1], gives rise to a voltage at the port of the corresponding antenna. Besides, inherent in each EM wave are frequency, amplitude as well as phase of it not to mention its time dependency. As a result, the voltage across the termination of our antenna is, at least, a function of frequency, time and spatial characteristics of both incoming EM waves and radiation far field function of the element. Based on the bases established in the preceding chapters, we reiterate that in the frame of our study, in order to focus on the performance of the terminal, we look upon them neither in time nor in frequency domain. Instead, we restrict ourselves to space domain and think of any antenna as a space filter, which receives EM waves available in a portion of space with certain efficiency. Yet, this assessment is at a specified frequency.

As mentioned, in a multipath and in particular a rich scattering environment, the received voltage at the port of the antenna varies fast with respect to frequency, space and

[1] It is already described in chapter 2.

time. Bear in mind that the time dependency meant here is irrelevant to time harmonic nature of the desired EM waves, which is accounted for by virtue of the phasor concept. We are interested in samples of the received signal at different moments and in order to leave no source of confusion to mix up space and time domains preferably attribute these samples to different scenarios.

At each scenario, there are finite number of EM plane waves, say K, each coming from arbitrary direction (i.e., AoA) being specified by its solid angle coordinates, shortly denoted by $\Omega(\theta, \psi)$. Many experimental results have shown that the amplitude of the received voltages at the ports of the elements comply with Rayleigh distribution [10, sec.1.1]. Since the voltages could be considered as a weighted sum of the incident electric fields upon the antenna, based on the central limit theorem, the incident electric fields could presumably be random variables of independent, identical distribution regardless of the precise forms of their distribution functions. In the frame of our work, for sake of convenience alone, a zero mean complex Gaussian random variable stands a brilliant model to be used for these incoming EM waves.

All these time-harmonic EM waves affiliated with the same scenario contribute to the final received voltage across the impedance termination on the port. Associated with this voltage phasor is also a time-averaged power, which is, like voltage, a function of the termination on the port too. The formulas governing this relations were derived and elaborated precisely in chapter 3. Yet, they need to be modified for a general case of several incoming EM waves. Thus, by virtue of superposition concept, we can rewrite (3.15) and (3.16)[2] as follows,

$$\boxed{P_{\mathrm{L}}^{i\,\mathrm{sc}} = \frac{\lambda^2}{4\eta^2\ P_{\mathrm{avs}}^{i}} \left| \sum_{k=1}^{K} \vec{G}_{\mathrm{emb}}^{i}(\Omega_k^{\mathrm{sc}}) \cdot \vec{E}_{\mathrm{inc}}^{\mathrm{sc}}(\Omega_k^{\mathrm{sc}}) \right|^2} \tag{4.1}$$

$$\boxed{V_{\mathrm{L}}^{i^{\mathrm{sc}}} = \frac{-2j\lambda}{\eta\ I^i} \frac{Z_{s_i}}{Z_{\mathrm{in}}^{i} + Z_{s_i}} \sum_{k=1}^{K} \vec{G}_{\mathrm{emb}}^{i}(\Omega_k^{\mathrm{sc}}) \cdot \vec{E}_{\mathrm{inc}}^{\mathrm{sc}}(\Omega_k^{\mathrm{sc}})} \tag{4.2}$$

in which all the pertinent parameters are the same as those given in chapter 3. Note that the superscript "sc" stands as an identity tag to show to which scenario the power and voltage samples belong; also recall that η goes for intrinsic impedance of the medium, and λ is the operational wavelength. Furthermore as a reminder, bear in mind that in the above equation, which holds for the general case of multi-port antennas, the far field function is subject to

$$P_{\mathrm{rad}} = \frac{1}{2\eta} \oint_{4\pi} (|G_\theta(\Omega)|^2 + |G_\psi(\Omega)|^2) d\Omega\ . \tag{4.3}$$

Now, in a different scenario, an independent set of incident waves associated with different AoAs are considered giving rise to another power sample. By repetition, say for N times, we can create a vector of received power samples, $\bar{P}$, and the associated voltage

[2] Refer to page 23.

one, $\bar{V}$, each element of which corresponds to a certain independent scenario,

$$\begin{aligned} \bar{P} &= [P^{\mathrm{sc}_1}, P^{\mathrm{sc}_2}, \ldots, P^{\mathrm{sc}_N}]^T, \\ \bar{V} &= [V^{\mathrm{sc}_1}, V^{\mathrm{sc}_2}, \ldots, V^{\mathrm{sc}_N}]^T. \end{aligned} \tag{4.4}$$

It should be clear that at each port, there would be the associated power and voltage vectors. Hence, the number of received vectors equals the number of present ports in a multi-element antenna system.

The mean or expected value of vector $\bar{P}$, denoted by $\mathbb{E}$, is the average of all power samples at different scenarios and can shortly be called mean received power, P_{rec}. That is,

$$P_{\mathrm{rec}} = \mathbb{E}(\bar{P}) \ . \tag{4.5}$$

As a critical point, bear in mind that in parallel to the antennas under test, a reference antenna has to be exposed to the same sets of incoming EM waves in different scenarios. The average received power of this known antenna is then used for power normalization purposes [29]. For simulation use, the reference antenna could be an ideal[3], isotropic, dual-port, dual polarized antenna. We stress that in a particular case of a rich isotropic scattering environment, the shape of the pattern of an element is irrelevant to its performance [10, pp 139], [30], [31]. Therefore, as long as it is compensated for the known efficiency of any element, it can be used as a reference antenna. However, validity of the latter is strictly limited to rich isotropic environments and shall not be generalized to non-uniform cases.

The processes described above establish the central part of MEST, which has been implemented in MATLAB environment. Beside different antenna parameters e.g., embedded far field functions, $\bar{\bar{Z}}$, $\bar{\bar{Z}}_s$, $\bar{\bar{V}}_s$ etc., one needs to point out the total number of scenarios, N, as well as the number of incoming EM waves in each scenario, K. The former is related to the accuracy of the simulation, whereas the latter can be thought of as associated with *richness* of a multipath environment. As an example, the more the number of scenarios, the closer the corresponding CDF curves to the converged CDF curve ones. Indeed, the accuracy based on the number of scenario is to a considerable extend detailed in [19]. Richness of an environment has been addressed in [32] and the interested reader is referred to it.

Upon realizing a sufficient number of scenarios, MEST creates the associated voltage and power vectors at each existing port. Later, the CDF curves can be plotted and different diversity gains be extracted from them as detailed in chapter 2. On the other hand, correlation can be achieved from (2.5) on page 12 with desired voltage vectors substituted in it. The envelope correlation can be attained from (2.6) on page 12 in which the corresponding power vectors are inserted. Under isotropic environment constraint, the radiation efficiency for each branch can be defined as the ratio between the mean received power at the pertinent port to that of an ideal single port reference antenna, $P_{\mathrm{rec}}^{\mathrm{ref}}$. That is,

$$e_{\mathrm{tot}}^{i} = \frac{P_{\mathrm{rec}}^{i}}{P_{\mathrm{rec}}^{\mathrm{ref}}} \ , \tag{4.6}$$

[3] It has a unit total (embedded) efficiency.

with P_{rec} defined as in (4.5). In case we use a dual-port ideal reference antenna, the total embedded radiation efficiency becomes twice of that given in (4.6). The reason resides on the fact that in isotropic environments the balanced polarization condition is presumed for the incoming waves and the mean received power by a dual-port, dual-polarized ideal reference antenna is twice of its single-port counterpart. Our numerical study shows clearly that the simulated total radiation efficiency is the same as that simulated by a full wave simulator. In this way, the current issue can stand as a numerical verification of the way these efficiencies are measured in any reverberation chamber measurements.

4.2 Capacity

One of the most appealing benefits in using MIMO systems is associated with significant enhancement in spectral efficiency rendered by them [33]. Utilizing multi-port antennas enables the system to present linear increase in spectral efficiency with respect to the number of the elements, which is -no doubt- a rewarding feature. The concept is well-established in different literature[4] and the interested reader is referred to them. But, the main goal here is to evaluate an upper bound ergodic capacity that can be obtained by a multi-element antenna system.

Based on the process explained in the previous section regarding the simulation of our received signals, we can establish the artificial channel matrix as follows. Let us assume for instance that there are N_{T} transmit antennas. Due to scattering environment the EM waves originating from each transmitter reach the, say, N_{R}-element receive antenna and create a voltage vector at each port. Signals from other transmitters also establish the sources for independent sets of EM waves giving rise to a separate set of voltage vectors at different ports. Finally, the corresponding voltage vectors can be stacked in a matrix, $\mathbf{H}_{N_{\text{R}}\times N_{\text{T}}}$, representing a special channel matrix as elaborated above.

Also, since the received signal-to-noise (SNR) ratio plays an important role in capacity, it necessitates a proper normalization of the channel matrix leading to independence of $\mathbf{H}$ and SNR [34]. A general formula for normalization of the channel matrix is provided in [35] which can be recast as

$$\bar{\bar{H}}_n = \bar{\bar{H}} \left[\frac{1}{N N_{\text{T}} N_{\text{R}}} \sum_{n=1}^{N} \|\bar{\bar{H}}_r\|_F^2 \right]^{-1/2} , \tag{4.7}$$

where $\|\cdot\|_F$ is the Frobenius norm and $\mathbf{H}_r$ refers to the channel matrix of the reference antenna simulated in the same N scenarios. Note that N_{R} refers to the number of the ports in our reference antenna. The ergodic (mean) capacity can, thus, be evaluated by [12, pp 331]

$$C = \mathbb{E}\left[\log_2 \left(\det \left(\bar{\bar{I}} + \frac{\text{SNR}}{N_{\text{T}}} \bar{\bar{H}}_n^H \cdot \bar{\bar{H}}_n \right) \right) \right] \text{ bps/Hz} , \tag{4.8}$$

in which $\cdot^H$ refers to Hermitian transpose, $\mathbb{E}$ denotes the expectation operator and $\bar{\bar{I}}$ goes for identity matrix.

[4] For instance, look at [1, Chap. 4] or [12, Chap. 10].

In the frame of our study, we use the ergodic capacity as a measure for characterization of our multi-element antenna. In the literature, another measure known as *outage capacity* [1, pp. 75] is also in use which falls beyond the scope of the current thesis. Yet, it should be said that based upon the data available in MEST, the latter can simply be implemented in it. In the following section, we deal with some simulation and measurement results achieved by our software.

4.3 Simulations and Measurements

In this part, we present some examples of simulation and measurements by virtue of MEST. The first example is associated with the Eleven antennas to be introduced soon. The second example is affiliated with the case of six-monopoles above a perfect electric conductor (PEC) ground plane. This multi-port antenna system has been the main concern of reference [15] and was later reflected and independently simulated in reference [36]. In each example, the results of our simulation will be compared with those achieved by different prevalent methods which are documented and published already. By that, we would like to verify MEST and show its robust bases and foundations.

4.3.1 Two-port Eleven Antenna

Eleven antenna is among ultra wide-band multi-element antennas, which has been developed for use as a feed in future radio telescopes [37]. Inasmuch as it is wide-band and has multiple ports, it stands as a fine example for verification of MEST. It is also brilliant for us due to the fact that, under certain project called ETECH by Nordic research organization, Eleven antenna has been measured by three different measurement methods which finally have presented excellent agreements with each other ([37, Figures 7-9]) lending the possibility of verification of MEST with different prevalent approaches.

The structure of the Eleven antenna is illustrated in Fig.4.1 in which the four port antenna can be converted to a two-port counterpart by virtue of two 180° hybrids with appropriate terminations, as detailed in [37, Figure 2]. In the frame of this thesis, we use the embedded far field function, measured in Technical University of Denmark (DTU), and realize correlation and diversity gains by virtue of MEST. Later, the outcomes will be compared with those of [37, Figure 7]. The measured far field function's solid angular resolution is $1^\circ \times 1^\circ$ in θ and ψ. The bandwidth of the antenna expands upon 2-8 GHz and the far field functions were measured at 0.1 GHz frequency step.

Fig.4.2 illustrates the absolute value of complex correlation[5] curves achieved based on different methods: The first curve is through MEST and by means of (2.5) on page 12, where the number of scatterers and scenarios are $K = 200$ and $Sc = 10^4$, respectively. The second curve belongs to correlation attained by pattern multiplication for an isotropic environment the square of which is given in (2.7) on page 12. The third curve is a plot of square root of envelope correlation introduced in (2.6) on page 12. Finally, the fourth curve is the one measured in Reverberation Chamber evaluated through ADG curves [37, Fig.7] and [37, eq. 2] in this reference.

[5] It is simply referred to as correlation.

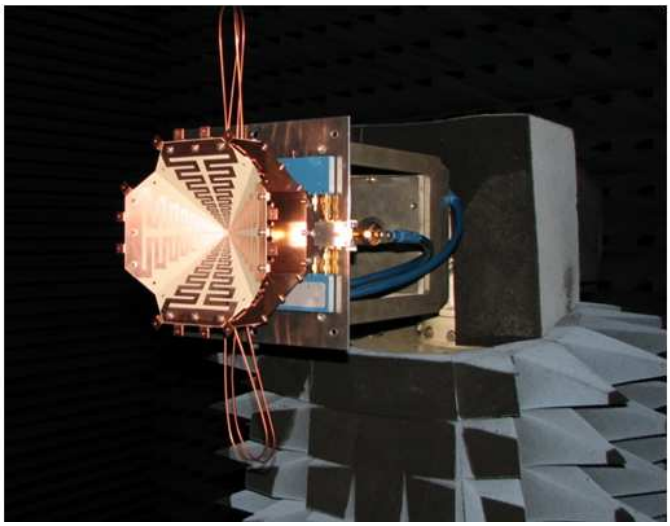

Figure 4.1: A picture of Eleven Antenna under test in Technical University of Denmark's anechoic chamber.

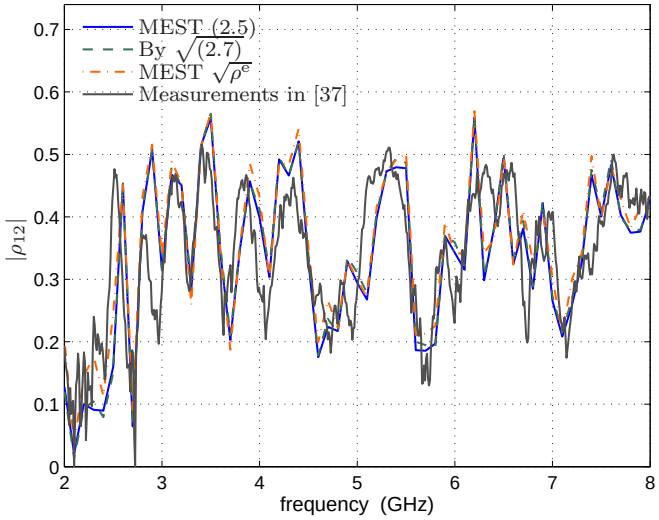

Figure 4.2: Correlation between the two ports of Eleven Antenna achieved by different methods over a wide bandwidth.

In the same way, we can achieve the ADGs by MEST, which is based on CDF curves of the received signals. On the contrary, knowing the correlation as well as total embedded radiation efficiencies, one may obtain the ADGs through closed-form formulas provided in [19]. Each ADG is associated with certain method. There are four different curves presented in Fig.4.3. Two of them are associated with ADG by CDF curves of the received signal created in MEST with $K = 200$ and $Sc = 10^5$. On the other hand, we have already shown that the correlation achieved in three different ways present a plausible agreement. Moreover, the total embedded radiation efficiencies have been studied to display also a fine agreement [37]. Hence, we choose one of them e.g., the ones from DTU measurements, and realize the ADGs by means of the aforementioned closed-form formulas from [19]. Thus, the two other curves are associated to these results. Note that if we use parameters

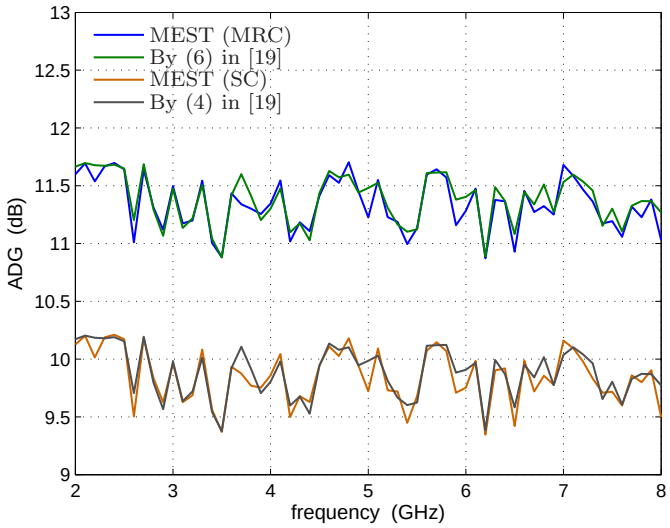

Figure 4.3: ADGs for MRC and SC schemes based on different methods. Those associated with MEST have been achieved by the corresponding CDF curves.

given from other methods, the resultant ADGs shall be -within certain accuracy- the same. The outcome, as observable, is brilliant verifying the results created by MEST.

4.3.2 Six monopoles on a PEC plane

In this section, we briefly turn our attention towards a case of six monopoles above a PEC ground plane which has been under analysis in the same way by two other references [15], [36]. The six-monopole radiation system has been a simple configuration commonly considered for adoptive and smart antennas, not to mention MIMO radiation terminals [15]. Fig.4.4 illustrates the configuration of this multi-element antennas, in which the six similar equidistant monopoles reside on a PEC, forming a hexagonal shape. Depending on the distance between the subsequent monopoles, the coupling and correlation between them as well as their total embedded efficiencies vary. We use a full wave simulator, called *Wire Structure Analysis Program* (WSAP) created by J. Carlsson, to achieve the S-parameters as well as the short-circuit embedded far field functions for each element.[6] Afterward, the $Z_\circ-$terminated embedded far field functions of them are evaluated.[7] Later, by means of MEST, a similar simulation as in [15] and [36] has been conducted, whose results are presented in Fig.4.5. These results are associated with the case where the distance between subsequent elements is $d = 0.14\lambda$.

The results show an acceptable agreement with each other despite the fact that there is a small discrepancy, in particular, between the curves associated with the case in which 3 transmit antennas are presumed. Yet, this small discrepancy can be attributed to some reasons. First of all, the far field solid angular resolution used in [36] is $3^\circ \times 3^\circ$ in θ and

[6] The mentioned full wave simulator is based on the method of moments for EM numerical computation.

[7] As a point of caution, it shall be said that the ground plane in WSAP extends to infinite while in practice it has a finite dimension.

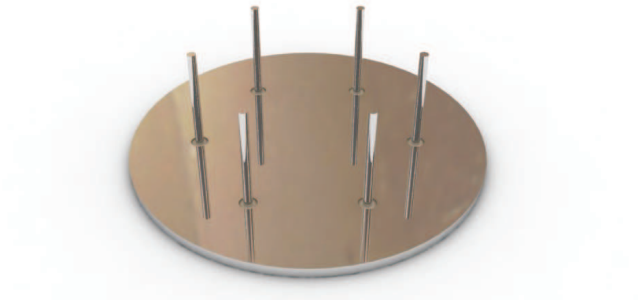

Figure 4.4: Six monopoles on a PEC ground plane. The distance between different elements is $d = 0.14\lambda$.

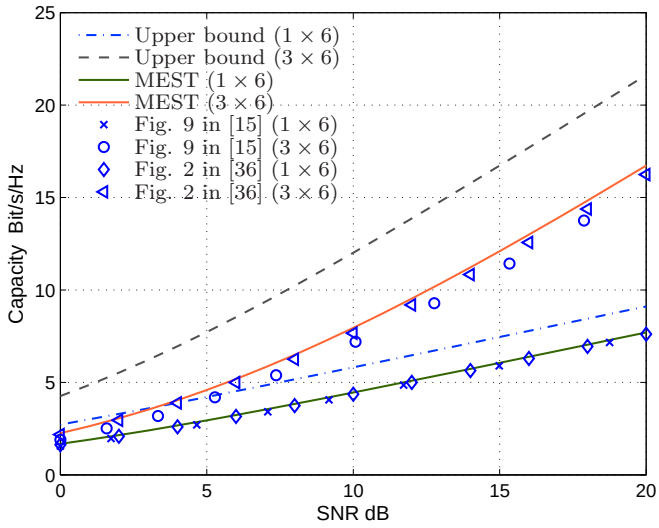

Figure 4.5: Simulation results for capacity of six-monopoles on a conducting ground plane with $d = 0.14\lambda$. Comparisons can be made with the corresponding results achieved in [15] (Figure 9) and [36] (Figure 2).

ψ whereas we used $1^\circ \times 1^\circ$ resolution. Moreover, the results are frequency dependent and a small shift in simulation frequency can be a major reason for this small disagreement. Above all, recall that the PEC dimensions in our simulations and those associated with the measured results are different. Finally, the total number of scenarios used in [15] and [36] is $Sc = 10^3$ while we used $Sc = 10^4$. Our choice was because to obtain a certain guarantee that the capacity achieved is not far from the converged one. We noticed that repetition of the same simulation for $Sc = 10^3$ results in a slight shift in the capacity curves which falls well within the disagreement we observe.

In addition to these two examples for verification of MEST, exclusive simulation and measurement results for this purpose have been presented in [32]. The interested reader is also recommended to read through this reference too.

4.4 Summary

In this chapter, we described the bases of our software, called MEST, which has been evolved upon the foundations developed in the preceding chapters. An exclusive and simultaneously brief part was dedicated to clarify the evaluation of capacity in this software. The latter followed by two examples in which the results produced by MEST were compared with those published in some renowned papers. The reader was also recommended to glance over reference [32] which presents some independent and brilliant measurement results for verification of MEST.

Chapter 5

Publications

This short chapter is dedicated to a brief overview of the appended papers. Independent abstracts from the ones given in each paper are presented here.

Paper I

Compact Formulas for Diversity Gains of Two-port Antennas

The main focus of this paper is on the dependency of the accuracy of ADG on the total number of independent measured samples either by setting up a measurement campaign in a multipath environment or through reverberation chamber measurements. The paper firstly conducts a study on the dependency of the relative error in estimation of ADG. It follows with motivating the fact that in a highly rich isotropic multipath environment, diversity gains are expressible through correlation and total embedded efficiencies. The paper consequently introduces two closed-from devised formulas rendering diversity gains of any arbitrary two-port antennas with acceptable accuracy. The two formulas are associated with a couple of renowned diversity combining schemes: SC and MRC.

Paper II

Performance of Directive Multi-element Antennas versus Multi-beam Arrays in MIMO Communication Systems

In a fairly precise way, the paper addresses the dependency of different MIMO parameters upon richness of a multipath environment and demonstrates a couple of examples for verification of the simulations. The simulation has been performed by means of MEST. For a case of rich isotropic environment, it is shown that the results of simulations comply brilliantly with those of measurements in a reverberation chamber. It is cleared that for a multi-port antenna system, in order to realize the optimum performance, an adequate number of incoming EM waves should exist.

Paper III

Study of Excitation on Beam Ports versus Element Ports in Performance Evaluation of Diversity and MIMO Arrays

In this paper, for the first time, we implement discrete Fourier transformation operation on received signals at the ports of a four-element antenna system. Discrete Fourier transformation on the received signals can be thought of as associated with rearrangement of the (omnidirectional) radiation patterns into directive beams oriented towards different directions in space, reminding the beam-forming technique. The paper, once more, illustrates that in a rich isotropic multipath environment the shapes of the patterns of the radiation elements are irrelevant to their ultimate MIMO performance.

Paper IV

Mode Counting in Rectangular, Cylindrical and Spherical Cavities with Application to Wireless Measurements in Reverberation Chambers

The main goal in this paper is to study the shape of the reverberation chambers as large resonant cavities on their performance as antenna measurement tools. It is known that an able reverberation chamber is the one rendering highest number of independent measured samples over a wide and continuous range of frequencies, in particular for those frequencies less than $f = 1$GHz. It can be shown that the latter is a feature of those cavities presenting a uniformly varying density of the EM resonance modes as a function of frequency. Bear in mind that the density of modes is evaluated within certain desired frequency windowing range.

Three types of cavities are of concerns which are compared and assessed based on the criterion as which one renders the most smoothly-varying density of modes over a certain range of frequencies. The paper finally concludes that the spherical reverberation chambers gives the reduced performance while rectangular and cylindrical ones exhibit more or less a similar and simultaneously attractive character. The paper deduces this inference that the more non-symmetrical the shape of the reverberation chamber is, the better would be the possibility of smooth variation in density of modes, and thus, the better is its ultimate performance as an antenna measurement tool.

Paper V

Effect of Mutual Coupling and Human Body on MIMO Performances

The paper is more focused on measurement of capacity and correlation for three different practical antennas. The paper once more demonstrates the undeniable fact that mutual coupling and correlation demolish the optimum performances of multi-port radiation terminals in multipath environments. Included are also some measurement results rendering

capacity at the presence of head phantom. The latter proves being effectively influential upon deterioration of the performance of a radiating antenna.

Bibliography

[1] A. Paulraj, R. Nabar, and D. Gore, *Introduction to Space-Time Wireless Communications*. Cambridge University Press, 2006.

[2] T. Aulin, "A modifed model for fading signal at the mobile radio channel," *IEEE Transactions on Vehicular Technologies*, vol. 28, no. 3, pp. 182–203, August 1979.

[3] T. Taga, "Analysis for mean effective gain of mobile antennas in land mobile radio environments," *IEEE Transactions on Vehicular Technology*, vol. 39, no. 2, pp. 117–131, 1990.

[4] K. Kalliola, K. Sulonen, H. Laitinen, O. Kiveks, J. Krogerus, and P. Vainikainen, "Angular power distribution and mean effective gain of mobile antenna in different propagation environments," *IEEE Transactions on Vehicular Technology*, vol. 51, no. 5, pp. 823–838, 2002.

[5] A. Kuchar, J.-P. Rossi, and E. Bonek, "Directional macro-cell channel characterization from urban measurements," *IEEE Transactions on Antennas and Propagation*, vol. 48, pp. 137–146, February 2000.

[6] H. Laitinen, K. Kalliola, and P. Vainikainen, "Angular signal distribution and cross-polarization power ratio seen by a mobile receiver at 2.15 ghz," *Proceeding of Millennium Conference on Antenna & Propagation, Davos, Switzerland*, April 2000.

[7] S. Qu and T. Yeap, "A three-dimensional scattering model for fading channels in land mobile environments," *IEEE Transaction on Vehicular Technologies*, vol. 48, pp. 765–781, May 1999.

[8] M. K. Ozdemir, E. Arvas, and H. Arslan, "Dynamics of spatial correlation and implications on MIMO systems," *IEEE Communications Magazine*, vol. 42, no. 6, pp. 14–19, 2004.

[9] Bluetest AB; http://www.bluetest.se.

[10] W. C. Jakes, *Microwave Mobile Communications*. John Wiley & Sons, 1974.

[11] G. Grimmett and D. Stirzaker, *Probability and Random Processes*, 3rd ed. Oxford, 2001.

[12] A. Goldsmith, *Wireless Communications*. Cambridge University Press, 2005.

[13] D. Tse and P. Viswanath, *Fundametals of Wireless Communication*. Cambridge University Press, 2008.

[14] A. F. Molisch, *Wireless Communications*. John Wiley & Sons, 2007.

[15] K. Rosengren and P.-S. Kildal, "Radiation efficiency, correlation, diversity gain and capacity of six monopole antenna array for a MIMO system: Theory, simulation and measurement in reverberation chamber," *Proceedings IEE, Microwaves Antennas and Propagation*, vol. 152, no. 1, pp. 7–16, 2005, see also Erratum published in August 2006.

[16] P.-S. Kildal and K. Rosengren, "Electromagnetic analysis of effective and apparent diversity gains of two parallel dipoles," *IEEE Antennas and Wireless Propagation Letters*, vol. 2, no. 1, pp. 9–13, 2003.

[17] ——, "Correlation and capacity of MIMO systems and mutual coupling, radiation efficiency and diversity gain of their antennas: Simulations and measurements in reverberation chamber," *IEEE Communication Magazine*, vol. 42, no. 12, pp. 102–112, 2004.

[18] P.-S. Kildal and C. Orlenius, *Chapter 58 in Antenna Engineering Handbook*, 4th ed., J. L. Volakis, Ed. McGraw-Hill, 2007.

[19] N. Jamaly, P.-S. Kildal, and J. Carlsson, "Compact formulas for diversity gain of two-port antennas," *IEEE Antennas and Wireless Propagation Letters*, vol. 9, pp. 970 –973, 2010.

[20] R. Ertel and J. Reed, "Generation of two equal power correlated rayleigh fading envelopes," *IEEE Communications Letters*, vol. 2, no. 10, pp. 276–278, October 1998.

[21] R. Vaughan and J. Andersen, "Antenna diversity in mobile communications," *IEEE Transactions on Vehicular Technology*, vol. 36, no. 4, pp. 149–172, November 1987.

[22] M. Ivashina, M. Kehn, P.-S. Kildal, and R. Maaskant, "Decoupling efficiency of a wideband vivaldi focal plane array feeding a reflector antenna," *IEEE Transactions on Antennas and Propagation*, vol. 57, no. 2, pp. 373–382, February 2009.

[23] C. A. Balanis, *Antenna Theory: Analysis and Design, 2nd Edition*. John Wiley & Sons, 1997.

[24] P.-S. Kildal, "Equivalent circuits of receive antenna in signal processing array," *Microwave and Optical Technology Letters*, vol. 21, no. 4, May 1999.

[25] D. K. Cheng, *Field and Wave Electromagnetics, Second Edition*. Addison-Wesley, 1989.

[26] R. E. Collin, *Antennas and Radiowave Propagation*. McGraw-Hill, 1985.

[27] K. Kurokawa, "Power waves and the scattering matrix," *IEEE Transactions on Microwave Theory and Techniques*, vol. 13, no. 2, pp. 194–202, March 1965.

[28] J. W. Wallace and M. A. Jensen, "Termination-dependent diversity performance of coupled antennas: Network theory analysis," *IEEE Transactions on Antennas and Propagation*, vol. 52, no. 1, pp. 98–105, January 2004.

[29] P. Suvikunnas, J. Salo, and P. Vainikainen, "Impact of power normalization in experimental MIMO antenna performance studies," *IEEE Antennas and Wireless Propagation Letters*, vol. 6, pp. 43–46, 2007.

[30] A. F. Molisch and X. Zhang, "FFT-based hybrid antenna selection schemes for spatially correlated MIMO channels," *IEEE Communication Letters*, vol. 8, no. 1, 2004.

[31] A. Grau, J. Romeu, S. Blanch, L. Jofre, and F. D. Faviis, "Optimization of linear multi-element antennas for selection combining by means of a Butler matrix in different MIMO environments," *IEEE Transactions on Antennas and Propagation*, vol. 54, no. 11, 2006.

[32] N. Jamaly, H. Zhu, P.-S. Kildal, and J. Carlsson, "Performance of directive multi-element antennas versus multi-beam arrays in MIMO communication systems," in *2010 Proceedings of the Fourth European Conference on Antennas and Propagation (EuCAP)*, April 2010, pp. 1–5.

[33] B. Holter, "On the Capacity of the MIMO Channel–A Tutorial Introduction," *Department of Telecommunications, Norwegian University of Science and Technology, Stavenger, Norway, Technical Report*, 2001.

[34] C. Waldschmidt, S. Schulteis, and W. Wiesbeck, "Complete RF system model for analysis of compact MIMO arrays," *IEEE Transactions on Vehicular Technology*, vol. 53, no. 3, pp. 579–586, May 2004.

[35] M. A. Jensen and J. W. Wallace, "A review of antennas and propagation for MIMO wireless communications," *IEEE Transactions on Antennas and Propagation*, vol. 52, no. 11, pp. 2810–2824, November 2004.

[36] K. Karlsson and J. Carlsson, "Analysis and optimization of mimo capacity by using circuit simulation and embedded element patterns from full-wave simulation," in *2010 International Workshop on Antenna Technology (iWAT)*, March 2010, pp. 1–4.

[37] J. Yang, S. Pivnenko, T. Laitinen, J. Carlsson, and X. Chen, "Measurements of diversity gain and radiation efficiency of the eleven antenna by using different measurement techniques," in *2010 Proceedings of the Fourth European Conference on Antennas and Propagation (EuCAP)*, April 2010, pp. 1–5.

Part II
Publications